JOURNAL OF MODERN OPTICS, 1991, VOL. 38, NO. 12, 2531–2541

Interferometric measurements of phase singularities in the output of a visible laser

A. G. WHITE, C. P. SMITH, N. R. HECKENBERG,
H. RUBINSZTEIN-DUNLOP, R. MCDUFF, C. O. WEISS
Department of Physics, The University of Queensland, St Lucia, Australia

and CHR. TAMM
Physikalisch-Technische Bundesanstalt, Braunschweig, Germany

(*Received 14 April 1991; revision 11 July 1991*)

Abstract. We report the use of a simple interferometric technique which allows direct identification of phase singularities in laser fields. Phase singularities are observed in families of optical patterns formed *via* cooperative frequency mode locking in a continuous single longitudinal mode Na_2 ring laser. The interferometric technique complements a previously reported astigmatic imaging method, and is superior in that it can be used to elucidate the structure of the higher order stationary patterns.

1. Introduction

Observations of transverse modal patterns in lasers are nearly as old as lasers themselves. Indeed, Goldsborough [1] presented a detailed study of the heterodyne interaction of multiple cavity eigenmodes in 1964. However, in recent times there has been renewed interest in the transverse modal behaviour of lasers. In [2], pattern formation *via* a mechanism known as multimode cooperative frequency locking was proposed. This was then extended to include realistic laser models in [3]. In this regime several cavity eigenmodes oscillate concurrently, but instead of interfering and producing a time-varying output pattern, as reported by Goldsborough, the transverse modes lock to a common frequency. As the relative phases of the cavity eigenmodes are fixed, the output intensity has a stationary transverse configuration.

It is possible for the phases to lock in such a way that there exist phase singularities or phase discontinuities within the stationary pattern. A phase singularity is defined as a point where the phase integral around a closed path surrounding the point is an integer multiple of 2π [4].

$$\oint \nabla\phi \cdot \mathrm{d}l = 2\pi m, \qquad \text{where } m = \pm 1,\ \pm 2,\ \pm 3, \ldots . \tag{1}$$

Here, $\nabla\phi$ is the gradient of the phase and $\mathrm{d}l$ is the line element on the closed path around the singularity. The integer m is called the topological charge of the singularity. At a singularity both the real and the imaginary parts of the electric field are zero, and it appears as an isolated dark spot within the observed intensity pattern.

Similarly patterns may exhibit phase discontinuities which appear as connected dark regions, again due to the zero-field components. However, in a phase discontinuity the overall topological charge is zero: there is an abrupt phase change of π radians across the line of the discontinuity. It is important to be able to distinguish between the two phase phenomena experimentally as both produce dark regions in the transverse intensity patterns.

In [5] an astigmatic imaging technique that indirectly identifies such phase phenomena is described. The technique was originally developed to reveal a 'hidden' bistability and explore switching in an optical laser. Multimode cooperative frequency locked laser systems exhibit multistability in that it is possible for the laser to output any one of a discrete set of stationary patterns under the same operating conditions. It is found that the low-order 'doughnut' pattern produced by cooperative mode locking is bistable. The doughnut equiphase surface is helical [6] and thus there are two patterns, one of right-hand and one of left-hand chirality, with identical transverse intensity profiles. The astigmatic imaging decomposes a symmetrical stationary pattern into an interference pattern between its constituent TEM_{10} and TEM_{01} modes. The interference patterns for the right and left hand chiralities are different and so this technique distinguishes between two patterns with identical transverse intensity profiles. It also indirectly identifies the central hole of the doughnut as a singularity, as only such a pattern decomposes in this manner.

The astigmatic imaging technique will give simple results only for cylindrically symmetric patterns. Furthermore it does not direcly map the singularities nor give information about the overall relationship between the singularities within the pattern. In a detailed theoretical and experimental treatment of pattern formation in a ring laser [7], it has been found that in many of the higher-order stationary patterns, there coexist singularities of opposing 'charge' leading to a low overall charge for the pattern. Although images of patterns with the dark regions placed as predicted by theoretical calculations were presented, the experimental results did not reveal the nature or charges of the singularities.

This paper describes the use of an interferometric technique for detection of singularities in stationary patterns. The method used is essentially that of [6] and we demonstrate here that it does indeed directly provide the location and charge of the phase singularities in stationary patterns. The principle of the method is set out in the next section, followed by a description of the experimental apparatus. The section immediately after that contains images of typical examples of stationary patterns and the interference patterns that reveal their structure. The final section discusses the applicability and extensions of this technique.

2. Theory

Stationary patterns can be treated as being composed of either Gauss–Laguerre or Gauss–Hermite cavity eigenmodes. Cooperative frequency locking occurs in situations of zero or negligible cavity astigmatism, situations that normally favour Gauss–Laguerre eigenmodes. Thus for simplicity, the detailed theoretical treatment in [7] treats the stationary patterns as consisting of various Gauss–Laguerre eigenmodes, although it is equally valid to use Gauss–Hermite modes.

The transverse mode patterns containing singularities are made up of two or more lower-order modal patterns which are active in the cooperatively frequency locked modal regime. The simplest singularity patterns consist of a TEM_{01} and a TEM_{10} modal patterns propagating together with a mutual phase difference of $\pi/2$. For such a pattern propagating in the z direction, the scalar electric field on some perpendicular screen can be written as:

$$\xi = \xi_0 \frac{r}{\omega}(\cos\theta \pm i\sin\theta)\exp(-r^2/\omega^2)\exp(-ikr^2/2R) + \text{c.c.}, \tag{2}$$

where k is the wave-number, r is the radial coordinate, ω is the spot size on the screen, and R is the radius of curvature of the wavefront. θ is the azimuthal coordinate, and the $\pm$ refers to the choice of chirality of the helical wavefronts. The quantities ω and R are linked through the standard relationships describing gaussian beam propagation.

Consider the interference between such a field and a uniform plane wave u, incident at a slight angle and described by

$$u = \exp(-ik_z z - ik_x x), \tag{3}$$

where $k^2 = k_z^2 + k_x^2$.

If for simplicity the radius of curvature R is assumed to be very large, as will usually be the case, it is easy to show that the equation for the boundaries between the light and dark fringes is

$$y = \mp x \tan k_x x. \tag{4}$$

The pattern formed is shown in figure 1 (*a*). The presence of a singularity is signalled by a defect in the fringe pattern where a new fringe starts. Observation of such defects provides a simple way to locate singularities experimentally. Away from the singularity we see a uniform pattern of straight fringes characteristic of two inclined plane waves. Higher-order singularities will manifest themselves with correspondingly larger numbers of extra fringes, and changing the sign of the singularity inverts the pattern.

Experimentally, rather than trying to produce a coherent plane wave to interfere with a given spot [8], it turns out to be easier to duplicate the spot using a beam splitter and then interfere the two spots together with a small mutual angle and displacement. The expected result for the case of the doughnut mode is shown in figure 1 (*b*, *c*). In both cases the singularity in each spot has been placed on the relatively uniform bright ring of the other, where the phase varies so slowly that it approximates a plane wave. These figures differ in the orientation of the interference fringes (which depends on the inclinations of the two beams) with respect to the line joining the singularities. In 1 (*b*) the fringes are vertical as in 1 (*a*), while in 1 (*c*) they are horizontal. In an experiment they might well adopt an intermediate angle, and if the distance between the singularities does not correspond to an integral number of fringes, the fringe bifurcations may be distorted, or a bright fringe may split rather than a dark one. These figures are immediately interpretable by comparison with figure 1 (*a*) as at each singularity location, a dislocation in the fringe pattern occurs and an extra fringe starts.

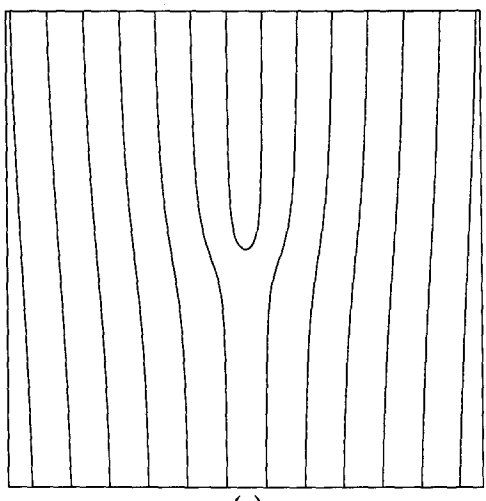

(*a*)

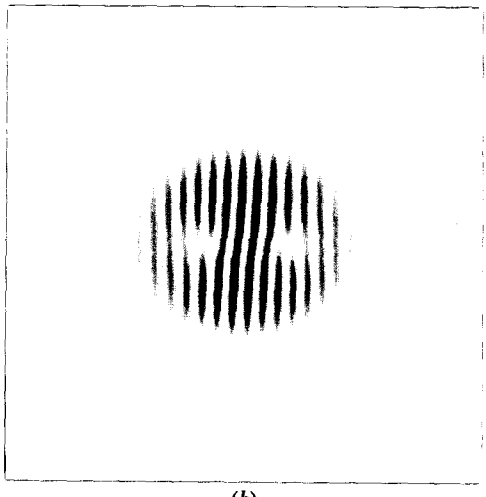

(*b*)

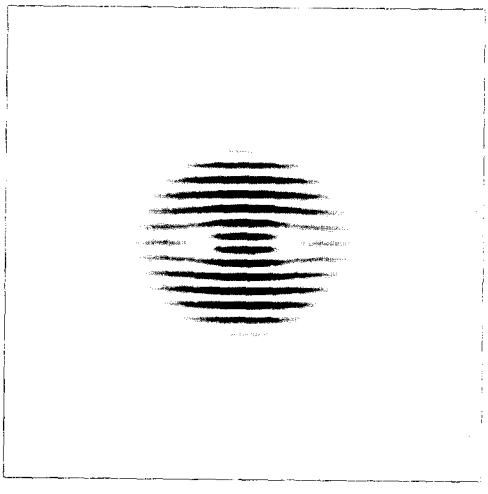

(*c*)

3. Experimental set-up

The experimental set-up is shown in figure 2. A similar experimental arrangement and details of the experimental conditions for the laser system have been described by Brambilla *et al.* [7]. The stationary patterns are produced by a sodium dimer vapour laser operating on the $\lambda = 525$ nm Q13 laser transition of Na_2. The Na_2 vapour laser is collinearly pumped by a Gaussian output beam from a frequency stabilised single longitudinal mode Ar ion laser operating at $\lambda = 488$ nm. The pump laser is tuned *via* an intracavity etalon to the centre of the Doppler-broadened (6,43) $X^1\Sigma_g^+$–(3,43) $B^1\Pi_u$ transition of Na_2. There are six strong lasing lines in this configuration: Q9–Q10 and Q13–Q16. An intracavity prism is used to select the strongest line. (The relative strengths of these lines vary with differing pump conditions and pure single line operation is not always achieved.) The sodium dimer vapour is produced and contained in a heat pipe with Brewster windows [9]. The heat pipe is operated at a temperature of 700 K, with a buffer gas of argon at a pressure of approximately 1–10 torr. Helium can be used as the buffer gas, but it is found to quench the lasing action to a greater degree than argon. Typical pump powers are in the range of 0·1–1·5 W, with the pump irradiance inside the cell thus varying between 0·1–1·5 MW m^{-2}. Unidirectional travelling-wave oscillation of a single longitudinal mode is observed under all operating conditions.

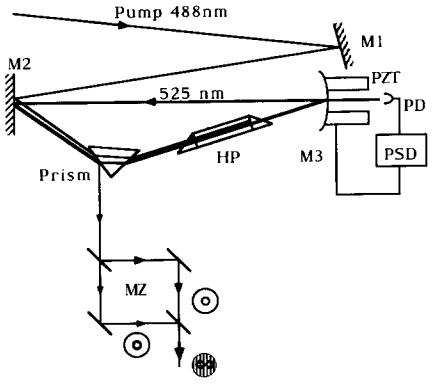

Figure 2. Experimental setup. The $\lambda = 488$ nm pump radiation is collimated by a telescope (not shown) which is adjusted so that the pump beam waist is approximately in the centre of the heat pipe (HP). The laser ring resonator is quasi-semiconfocal and consists of: a high reflectance plane mirror M2; a high-reflectance concave mirror, M3, of radius of curvature of 75 cm; a high-dispersion intracavity prism; and two intracavity Brewster windows attached to the heat pipe. The intracavity Brewster windows ensure that $\lambda = 525$ nm radiation is uniformly linearly polarised. The intracavity prism selects a particular molecular transition as the lasing transition and corrects for the astigmatism introduced by the windows. The photodiode detector PD, phase sensitive detector PSD, and piezoelectric mirror translator PZT form a feedback loop that locks a given high-order cavity eigenmode to the maximum of the gain line of the active medium.

Figure 1. (*a*) Boundary formed between light and dark fringes at a phase singularity as described by equation 4. (*b*) Theoretical plot of interference pattern produced by interferometer with a charge one 'doughnut' pattern as input. Note the termination of a fringe at each point where a singularity exists. (*c*) As 1 (*b*) but with beam directions adjusted to produce horizontal interferences fringes rather than vertical.

The laser cavity is quasi-semiconfocal: i.e. the radius of curvature of mirror M3 and the optical round trip path of the cavity are equal (figure 2). The quasi-semiconfocality ensures that the Gauss–Laguerre TEM_{spl} modes of transverse order $2p+l=q$ $(q=0,1,2,3)$ are equally spaced between adjacent axial modes, for example, TEM_{s00} and $TEM_{(s+1)00}$. In this relationship p and l are the radial and azimuthal indices respectively. This configuration also causes higher-order eigenmodes of order $2p+l=4k+q$ $(k=1,2,\ldots)$ and longitudinal order $s-k$ to become frequency degenerate with modes of order $2p+l=q$ and longitudinal order s. This would be a complication, were it not for the limited gain cross-section ensuring that these higher-order modes do not oscillate. Experimentally, it is found that with a radius of curvature of 750 mm the optical path length of the cavity only has to agree to within ± 15 mm to satisfactorily separate the four families of modes corresponding to different values of q.

For the purposes of pattern formation it is desirable that the differences between losses for the various cavity eigenmodes are insignificant. This is achieved in a high-loss high-gain cavity where mode independent losses, such as the outcoupling losses, dominate. The high gain provided by the Na_2 vapour is necessary simply to overcome the high losses and allow lasing operation.

In this set-up cavity losses occur at the mirror and prism surfaces. These losses provide a number of output beams for use, one of which is monitored with a photodetector to generate a signal for the feedback stabilisation system. This system serves to adjust the cavity length to maximize the power of a modal pattern. If the laser is not operating in the cooperative frequency locked multimode regime then a beat frequency between 1–10 MHz is observable in the photodetector signal.

The main output beam is directed into a Mach–Zehnder interferometer, which consists of two mirrors and two beam splitters arranged to form a rectangle. This configuration is preferred over a Michelson interferometer as it reduces the amount of light which is fed back into the laser cavity ensuring that the modal patterns are not perturbed in any way. The interferometer is adjusted so that the spots from the two arms are slightly misaligned. The degree of misalignment can be adjusted to decrease or increase the spacing of the fringes by rotating the mirrors in either the x or y directions. This allows clear observation of each singularity (as explained in the next section). The output from the interferometer is displayed on a screen and recorded using an EDC-1000 CCD camera. The CCD camera has a greater dynamic range (60 dB) than film and thus avoids image saturation. Images are obtained *via* a 192 by 165 pixel array which has a 256 level gray scale intensity resolution. Adequate picture quality is obtained with exposure times on the order of 200–500 ms. The images can be viewed in a photographic format or converted to graphical form for a more quantitative comparison with theory.

4. Results

Altering the length of the cavity by fractions of a micrometre allows access to four frequency degenerate families of modes. As explained above, these fulfill the condition $2p+l=q$ $(q=0,1,2,3)$. Stationary patterns consist of phase locked combinations of members of each family of Gauss–Laguerre modes. The families produce one, two, four, and six stationary patterns respectively. The $2p+l=0$ case is simply the lowest-order Gaussian mode, with no singularities. The $2p+l=1$ family consists of a doughnut pattern with a singly charged singularity. There are in fact two

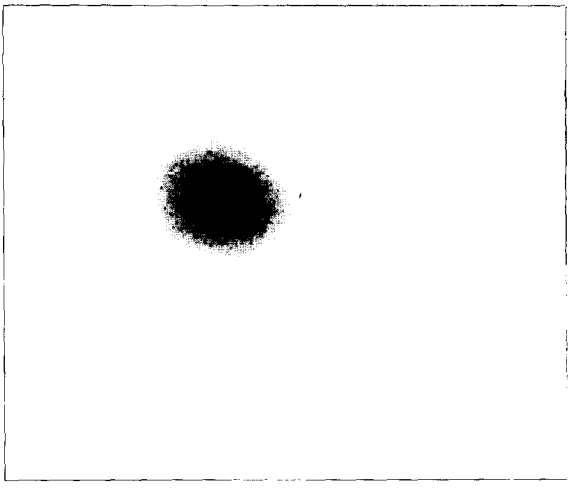

(*a*)

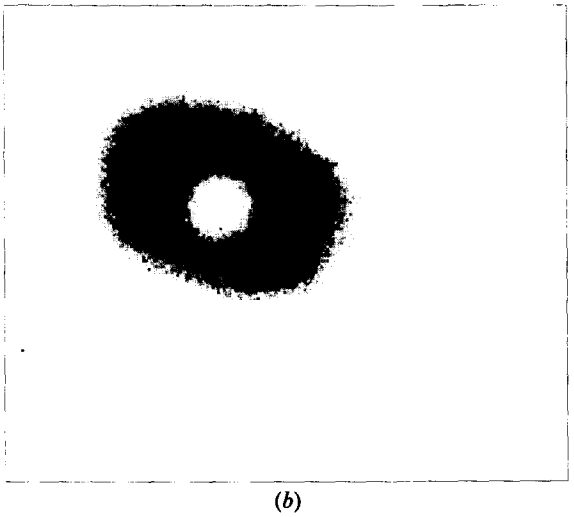

(*b*)

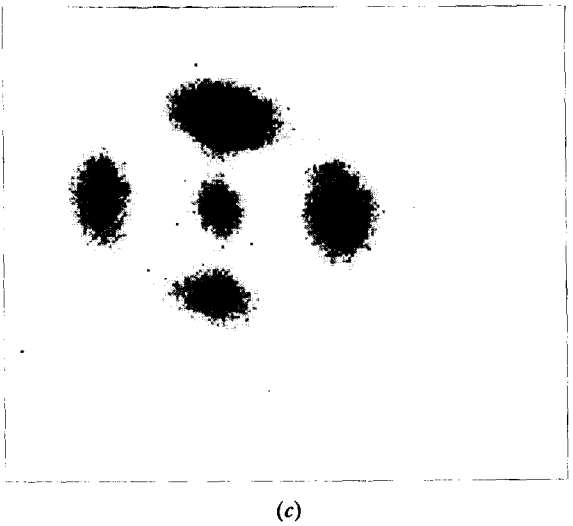

(*c*)

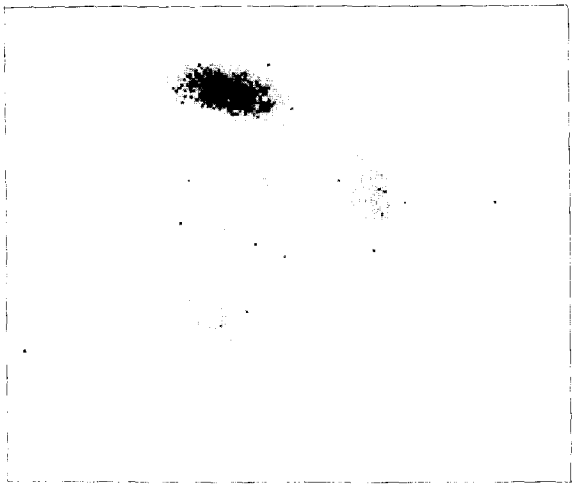

(*d*)

Figure 3. The images in figure 3 (*a–d*) were produced by maintaning constant operating conditions and varying the cavity length so as to scan through the mode families. (*a*) A Gaussian pattern from the $2p+l=0$ family. (*b*) A charge one doughnut pattern from the $2p+l=1$ family. (*c*) A four-spot or 'leopard' pattern from the $2p+l=2$ family. (*d*) A five-spot pattern from the $2p+l=3$ family.

solutions as the singularity has two possible signs. These solutions are bistable [5]. The $2p+l=2$ and $2p+l=3$ families contain stationary patterns of more complex shape, some containing no singularities while others contain multiple or higher-order singularities. These patterns exhibit a complicated multistability [5, 7, 10].

Figure 3 (*a–d*) are CCD camera images of a Gaussian pattern, a charge one doughnut, the 'leopard' or four-spot pattern, and a five-spot pattern respectively. These were obtained by maintaining constant operating conditions and varying the cavity length to obtain a stationary pattern from each family. According to [7] there are two negatively and two positively charged singularities in the leopard, all of charge one, placed so that the like charges are diagonally opposite one another. In the five-spot it is proposed that a square of four like, singly charged, singularities surround a singularity of opposite charge.

Figure 4 (*a*) is the interference pattern of the $2p+l=0$ Gaussian pattern. As there is no singularity the interference pattern obtained consists simply of straight fringes, the inclination and spacing of which depend on the orientation of the interferometer mirrors. In contrast to this is figure 4 (*b*), which is the interference pattern formed by the 'doughnut' stationary pattern from the $2p+l=1$ family. Note that the interferometer mirrors have been adjusted so that images produced by each interferometer arm are slightly displaced. It can be clearly seen that an interference fringe terminates at each of the 'doughnut holes', proof of a phase singularity at that location. Furthermore, the charge of the singularity is confirmed by the number of terminating fringes. As there is only one at each singularity the doughnut is a charge one, or $2p+l=1$ family doughnut. There is good agreement between figure 4 (*b*) and the theoretical prediction for this case shown in figure 1 (*b, c*).

The pattern shown in figure 5 (*a*) is clearly related in some manner to the $2p+l=3$ family five-spot stationary pattern, although it is grossly distorted both in

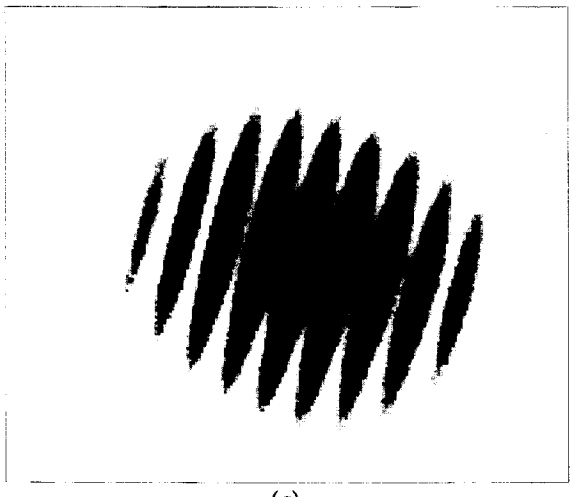

(*a*)

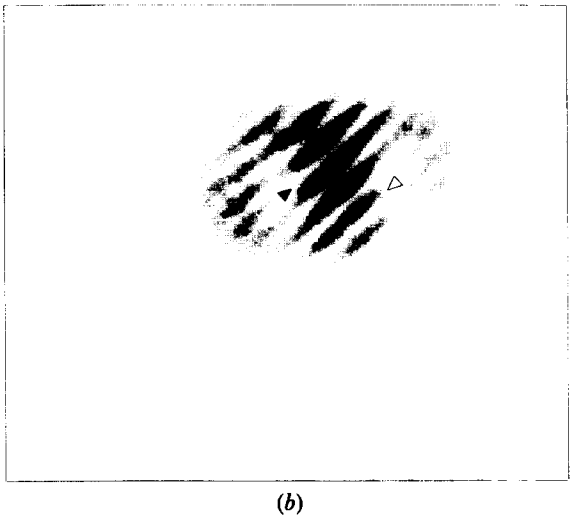

(*b*)

Figure 4. Figure 4 (*a*, *b*) are interferograms produced with the Mach–Zehnder interferometer. (*a*) Interferogram of a Gaussian pattern. (*b*) Interferogram of a doughnut pattern. The single fringe terminations reveal the doughnut is charge one.

shape and intensity compared to the 'classic' five-spot shown in figure 3 (*d*). The astigmatic distortion in shape is due mainly to the observational screen being placed at an oblique angle to the transverse cross-section of the beam. The astigmatic distortion in intensity, i.e. the two very bright outer spots or 'outriders', is due to a slight intracavity asymmetry. A theoretical interferogram of two five-spots is shown in figure 5 (*b*). The question of whether figure 5 (*a*) is really a five-spot stationary pattern is thus answered by the experimental interferogram shown in figure 5 (*c*). As indicated on the figure, the characteristic array of four like charged singularities surrounding the central singularity of opposite charge is quite evident. Figure 5 (*c*) also provides direct confirmation of the theoretical charge distribution proposed for the five-spot pattern.

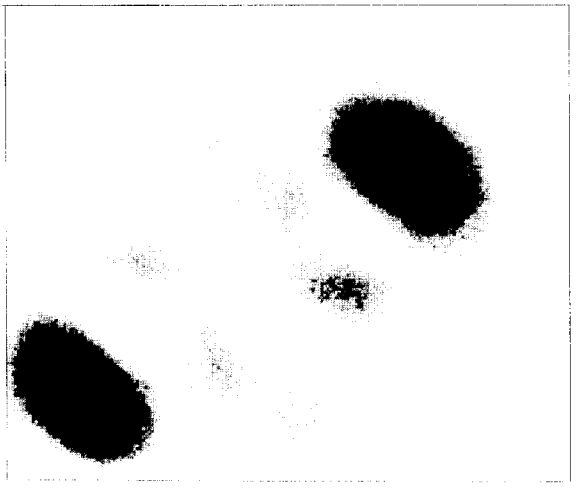

(*a*)

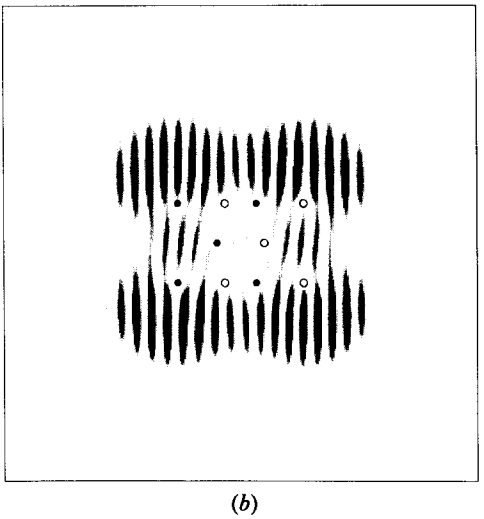

(*b*)

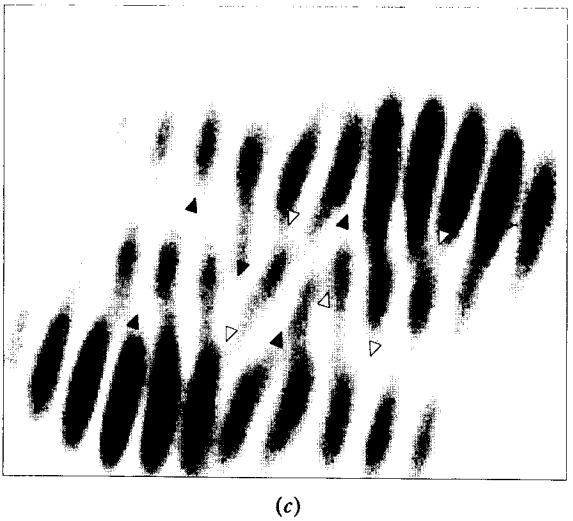

(*c*)

The relative charge of a given singularity can be ascertained by the incident direction of the terminating fringes. If the terminating fringe is considered as an arrow, with its head at the singularity, then within a pattern all singularities of like charge have terminating fringes pointing in the same direction, whereas singularities of opposite charge point in the opposite direction. It is also worth noting at this point that when using two-pattern interferograms two charges in equivalent positions in each pattern will have opposite signs. This is evident in figures 1 (*b*, *c*), and 5 (*b*, *c*). We find it is easy enough to identify which singularity belongs to which pattern by referring to recordings of the two interfering patterns made separately (like figure 5 (*a*)).

5. Conclusions

The existence of phase singularities has been suggested and indirectly shown previously by other groups, but no satisfactory method for their detection has been demonstrated. The interferometric technique outlined provides information both on the position and relative charge of singularities within a given stationary solution, and differentiates between phase discontinuities and phase singularities. A variety of patterns has been investigated, and despite distorted input patterns it has been shown that this technique will accurately identify the stationary solution.

For studies of very complex patterns it would probably be worthwhile to generate a uniform plane or spherical reference wave by spatial filtering of the laser output. This would halve the number of singularities in the inteference pattern and simplify analysis.

Acknowledgment

This work was supported by the Australian Research Council.

References

[1] GOLDSBOROUGH, J. P., 1964, *Appl. Optics*, **3**, 267.
[2] LUGIATO, L. A., OLDANO, C., and NARDUCCI, L. M., 1988, *J. opt. Soc. Am.* B, **5**, 879.
[3] LUGIATO, L. A., OPPO, G. L., TREDICCE, J. R., NARDUCCI, L. M., and PERNIGO, M. A., 1990, *J. opt. Soc. Am.* B, **7**, 1019.
[4] COULETT, P., GIL, L., and ROCCA, F., 1989, *Optics Commun.*, **73**, 403.
[5] TAMM, CHR., and WEISS, C. O., 1990, *J. opt. Soc. Am. B*, **7**, 1034.
[6] VAUGHAN, J. M., and WILLETS, D. V., 1983, *J. opt. Soc. Am.*, **73**, 1018.
[7] BRAMBILLA, M., BATTIPEDE, F., LUGIATO, L. A., PENN, V., PRATI, F., TAMM, C., and WEISS, C. O., 1991, *Phys. Rev.* A, **43**, 5090 and 5114.
[8] BARANOVA, N. B., ZEL'DOVICH, B. YA., MAMAEV, A. V., PILIPETSKIL, N. F., and SHKUKOV, V. V., 1981, *Soviet Phys. JETP*, **33**, 195.
[9] WELLEGEHAUSEN, B., 1979, *I.E.E.E. J. quant. Electron*, **QE-15**, 1108.
[10] LUGIATO, L. A., PRATTI, F., NARDUCCI, L. M., and OPPO, G. L., 1989, *Optics Commun.*, **69**, 387.

Figure 5. (*a*) A distorted five-spot pattern. (*b*) A theoretical two-pattern interferogram of the five-spot stationary solution. The positions of the singularities belonging to the two patterns are indicated, with a square of singly charged singularities surrounding another of opposite sign in each pattern. (*c*) An experimental two-pattern interferogram of figure 5 (*a*). Note the similarity to figure 5 (*b*). The positions of the intensity minima in the two interfering patterns are shown with symbols which indicate the incident direction of the corresponding terminating fringes associated with the singularities.